Efficient Methods for Hall Factor and Transport Coefficient Evaluation for Electrons and Holes in Si and SiGe Based on a Full-Band Structure

C. Jungemann, M. Bartels, S. Keith, and B. Meinerzhagen

Institut für Theoretische Elektrotechnik und Mikroelektronik
Universität Bremen, Kufsteiner Straße, Postfach 33 04 40, 28334 Bremen, Germany
Tel.: +49 421 218 4861, Fax: +49 421 218 4434, E-Mail: junge@item.uni-bremen.de

1. Introduction

The recent development in full-band Monte Carlo (FB-MC) methods has not only shown that FB-MC codes can be as efficient as analytical-band programs [1, 2], but also that the FB-structure is indispensable in the case of hot-electron simulations [3, 4]. In the case of holes the warped band structure makes analytical-band modeling very difficult even in equilibrium, and the use of the FB-structure is mandatory. The advent of new materials like SiGe necessitates the extensive calibration of the FB-MC codes with experimental data measured close to or in equilibrium [5], where standard MC-methods are notoriously inefficient. In this work methods are presented, which allow the efficient calculation of equilibrium and near-equilibrium transport properties in conjunction with an FB-structure evaluated by a nonlocal empirical pseudopotential method [6]. These methods are not only applied to the case of transport parameter calibration, but are also used for the extraction of transport coefficients for hydrodynamic models.

2. K-space grid

The FB-structure is discretized with a nonuniform tetrahedral grid in $\boldsymbol{k}$-space, which is generated with an adaptive method somewhat similar to [1, 7]. For each energy band a grid is generated starting with the basic tetrahedra of the irreducible wedge. The tetrahedra are refined until the maximum error in the linear interpolation of the energy along all edges of the tetrahedra is less than 2 % of the energy at the center of the respective edge or less than 0.05 meV, whatever is larger. Furthermore, the maximum length of an edge of a tetrahedron must be less than one tenth of the distance from Γ to X in the Brillouin zone. In Fig. 1 the grids of the first conduction and valence band are shown, which are extremely dense in the vicinity of the band minima to allow transport calculations at temperatures as low as 50 K. The minimum length of an edge of a tetrahedron is 0.0003 times the distance from Γ to X. The average quality of the tetrahedra according to [7] is 0.28.

To achieve a continuous energy interpolation over the whole $\boldsymbol{k}$-space the $LUWK$-surface of the irreducible wedge is discretized with a symmetric grid with respect to the LW-line (Fig. 2). This is necessary since particles, which change the Brillouin zone via this surface, appear in the adjacent wedge at a position which is on the opposite side of the LW-line compared to the initial position. To avoid a discontinuity in the energy interpolation the grid must have the same symmetry property as the band structure.

3. Mass tensor discretization

The inverse mass tensor is needed for hydrodynamic models [8] and for the evaluation of transport coefficients. The important point here is that the discretization of the inverse mass tensor on the nonuniform grid must be consistent with the interpolation of the energy band structure, which is linear within a tetrahedron and continuous at the interfaces of the tetrahedra. Based on the theorem of Gauß it can be shown that the integral of the inverse mass tensor $\underline{\underline{m}}^{-1}$ over the volume V_{tet} of a tetrahedron equals the integral of the group velocity $\boldsymbol{v}$ over the surface F_{tet} of the tetrahedron:

$$\frac{1}{V_{\text{tet}}}\int_{V_{\text{tet}}}\underline{\underline{m}}^{-1}\,\mathrm{d}V=\frac{1}{\hbar V_{\text{tet}}}\oint_{F_{\text{tet}}}\boldsymbol{v}\,\mathrm{d}\boldsymbol{F}^{\mathrm{T}}=\underline{\underline{m}}_{\text{tet}}^{-1}\ ,$$

where the inverse mass tensor and the velocity are defined as:

$$\underline{\underline{m}}^{-1}=\frac{1}{\hbar}\nabla_{\boldsymbol{k}}\boldsymbol{v}^{\mathrm{T}}\ ,\ \boldsymbol{v}=\frac{1}{\hbar}\nabla_{\boldsymbol{k}}\varepsilon\ .$$

Since the energy is linearly interpolated within a tetrahedron, the velocity is constant within a tetrahedron and discontinuous in the interface between two tetrahedra. Therefore the arithmetical mean of the velocities on both sides of the interface is used for the velocity within the interface. This yields for each tetrahedron a symmetric inverse mass tensor consistent with the discretized band structure. In Fig. 3 the expected value of the inverse mass tensor is shown for electrons and holes in undoped relaxed silicon at room temperature as a function of the electric field.

4. Calculation of transport parameters

With the microscopic relaxation time (MRT) it is possible to solve the one-particle Boltzmann equation exactly within the first order of the electric and magnetic field [9, 10]. For nondegenerate systems the MRT $\underline{\underline{\tau}}$ is

0-7803-4369-7/98 $10.00 ©1998 IEEE

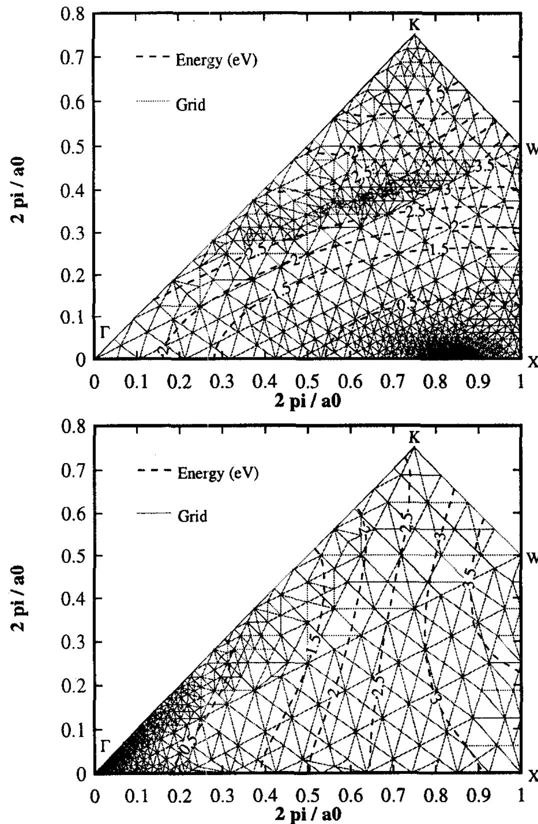

Fig. 1: Nonuniform adaptive tetrahedral grid of the first conduction band (upper graph) and of the first valence band (lower graph) in the k_x, k_y-plane of relaxed silicon.

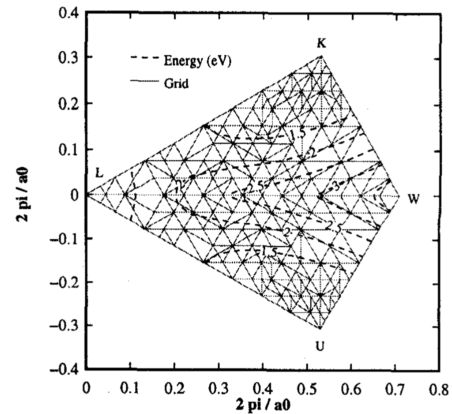

Fig. 2: Symmetric grid of the $LUWK$-plane of the first conduction band of relaxed silicon.

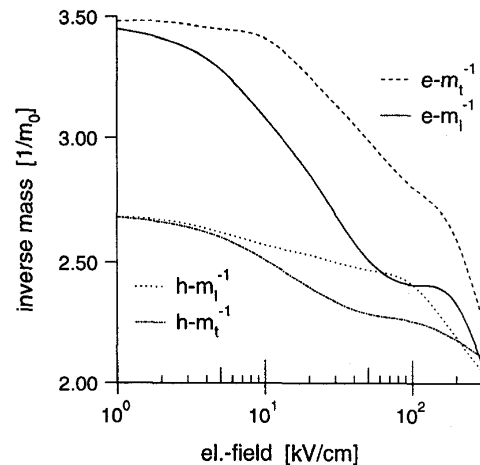

Fig. 3: Longitudinal and transversal inverse mass for electrons and holes in undoped silicon at room temperature as a function of the electric field in $\langle 100 \rangle$-direction.

defined by the integral equation [9] (Ω: system volume, $S(\boldsymbol{k}'|\boldsymbol{k})$: transition rate):

$$\boldsymbol{v}(\boldsymbol{k}) = \frac{\Omega}{(2\pi)^3} \int S(\boldsymbol{k}'|\boldsymbol{k}) \left[\underline{\underline{\tau}}(\boldsymbol{k})\, \boldsymbol{v}(\boldsymbol{k}) - \underline{\underline{\tau}}(\boldsymbol{k}')\, \boldsymbol{v}(\boldsymbol{k}') \right] \mathrm{d}^3 k' .$$

Due to the employed scattering models [5] the in general tensor-valued MRT is here only an energy-dependent scalar. Please note that this is exact for our FB-MC model in the case of holes, whereas it is a very good approximation in the case of electrons.

With the MRT the mobility and diffusion tensor can be calculated as expected values of the distribution function ($\langle\rangle$) for *arbitrary* electric fields [11]:

$$\underline{\underline{\mu}} = e \left\langle \tau \underline{\underline{m}}^{-1} + \frac{\mathrm{d}\tau}{\mathrm{d}\varepsilon} \boldsymbol{v}\boldsymbol{v}^{\mathrm{T}} \right\rangle , \quad \underline{\underline{D}} = \left\langle \tau \boldsymbol{v}\boldsymbol{v}^{\mathrm{T}} \right\rangle ,$$

where e is the electron charge. In the case of an additional *arbitrary* magnetic field the drift velocity can be evaluated by (neglecting quantum effects):

$$\langle \boldsymbol{v} \rangle = e \left\langle \left(\tau \underline{\underline{m}}^{-1} + \frac{\mathrm{d}\tau}{\mathrm{d}\varepsilon} \boldsymbol{v}\boldsymbol{v}^{\mathrm{T}} \right) \boldsymbol{E} + \tau \underline{\underline{m}}^{-1} (\boldsymbol{v} \times \boldsymbol{B}) \right\rangle ,$$

where in the calculation of the distribution function the magnetic field must be considered. However, the inclusion of a magnetic force in the FB-MC simulation is rather simple, because the velocity is constant within a tetrahedron due to the linear interpolation of the energy.

In Fig. 4 the mobilities and diffusion constants are shown as a function of the electric field for a strained silicon layer on a relaxed $\mathrm{Si}_{0.7}\mathrm{Ge}_{0.3}$ substrate. In the case of equilibrium the deviation from the Einstein relation is less than 0.5 % demonstrating the high quality of the discrete representation of the inverse mass tensor.

The drift velocity can be either estimated directly from the FB-MC simulation by averaging the particle velocity or by sampling the longitudinal mobility. In Fig. 5 the ratio of the CPU times of both cases is shown, when the simulation is stopped at 1% simulation error [12] for the longitudinal mobility or the drift velocity, whatever is smaller. In the case of electrons (holes) the estimator based on the above given formula for the mobility is much

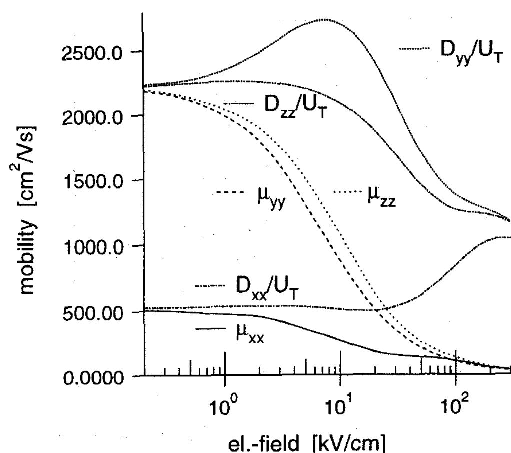

Fig. 4: Mobilities and diffusion constants (divided by $U_T = k_{\mathrm{B}}T/e$, $T = 300K$) for electrons in an undoped strained silicon layer in the (100)-plane on a relaxed $\mathrm{Si}_{0.7}\mathrm{Ge}_{0.3}$ substrate as a function of the electric field in [010]-direction.

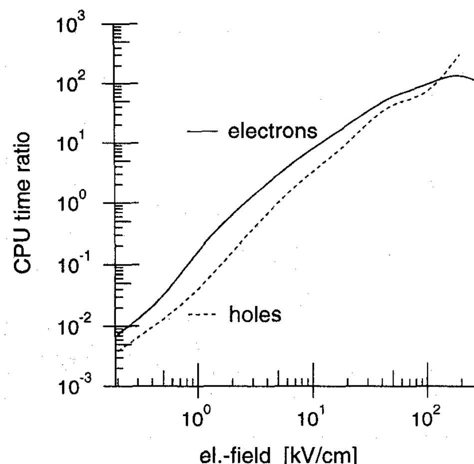

Fig. 5: Ratio of the CPU times needed to achieve the same simulation error by sampling the longitudinal mobility and by sampling the drift velocity directly from the MC-simulation for undoped silicon at room temperature.

more efficient than the direct sampling of the drift velocity for electric fields below 3 kV/cm (5 kV/cm), because it is based on even moments of the distribution function in contrast to the drift velocity, which is based on odd moments. Similar results are obtained for other transport parameters of hydrodynamic models like energy current. Thus it is possible to sample transport parameters efficiently in the "warm"-electron regime, where standard estimators are inefficient.

Since in most experiments the low-field Hall mobility instead of the drift mobility is measured, an efficient method for the calculation of the Hall factor in equilibrium is required. The corresponding equation for the Hall factor in the case of a small electric and small magnetic field under nondegenerate conditions reads [10, 13]:

$$r_{\mathrm{H}} = \frac{e^2}{k_{\mathrm{B}}T} \frac{(\boldsymbol{B} \times \boldsymbol{E})^{\mathrm{T}} \left\langle \tau^2 \underline{\underline{m}}^{-1} (\boldsymbol{v} \times \boldsymbol{B}) \, \boldsymbol{E}^{\mathrm{T}} \boldsymbol{v} \right\rangle_{\mathrm{eq}}}{B^2 \left(\boldsymbol{E}^{\mathrm{T}} \underline{\underline{\mu}} \boldsymbol{E} \right)^2 / E^2} ,$$

where eq denotes the equilibrium distribution function and $k_{\mathrm{B}}T$ is the thermal energy. In Fig. 6 the Hall factor is shown for undoped silicon as a function of the temperature. In addition, in Fig. 6 the Hall factor for holes is shown based on an FB-structure calculated with the local empirical pseudo potential method (LEP) [14] in contrast to the other results, which are based on the nonlocal empirical pseudopotential method (NLEP) [6]. While the differences are negligible in the case of electrons, a large difference is found for holes. Moreover, for a comparison simulation results from a previous work are shown, which are based on the $\boldsymbol{k} \cdot \boldsymbol{p}$–method [13].

In the case of equilibrium the distribution function is given by the Boltzmann distribution, and it is possible to calculate the Hall factor and the mobility consistent with the FB-structure using fast numerical integration instead of the MC-method. This facilitates rapid calculation of transport quantities necessary for transport parameter extraction from experiments, which are most often done under equilibrium or near-equilibrium conditions. In Fig. 7 the low-field electron mobility in a strained $\mathrm{Si}_{1-x}\mathrm{Ge}_x$ layer on a relaxed substrate is shown for different Ge-contents at 77K.

5. Conclusions

We have presented a method for the calculation of the inverse mass tensor which is consistent with the nonuniformly discretized band structure. The band structure is discretized in such a way that the grid is fine enough for transport calculations at 50K without an excessive total number of grid nodes. Based on these results estimators for the Hall factor and basic transport properties are given, which are more efficient in equilibrium and in the "warm"-electron regime than standard estimators.

References

1. J. Bude and R. K. Smith: Semicond. Sci. Technol. **9** (1994) 840.

2. C. Jungemann, S. Yamaguchi, and H. Goto: *Proc. ESSDERC* No. 26 (1996) p.821.

3. A. Abramo, L. Baudry, R. Brunetti, R. Castagne, M. Charef, F. Dessenne, P. Dollfus, R. Dutton, W. L. Engl, R. Fauquembergue, C. Fiegna, M. V. Fischetti, S. Galdin, N. Goldsman, M. Hackel, C. Hamaguchi, K. Hess, K. Hennacy, P. Hesto, J. M. Higman, T. Iizuka, C. Jungemann, Y.Kamakura, H. Kosina, T. Kunukiyo, S. E. Laux, H. Lin, C. Maziar,

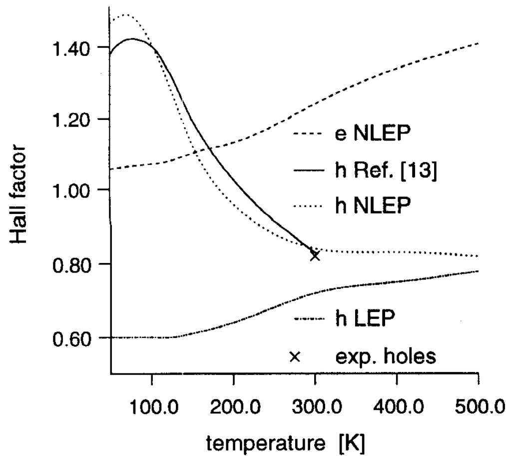

Fig. 6: Simulated Hall factors for electrons and holes (LEP-FB, NLEP-FB) in undoped relaxed silicon, an experimental result [15] and simulation results for holes from [13].

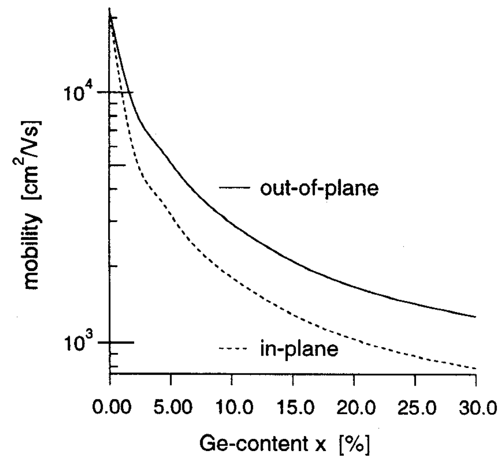

Fig. 7: In-plane and out-of-plane electron mobility in an undoped strained $Si_{1-x}Ge_x$ layer on a relaxed silicon substrate at 77K.

H. Mizuno, H. J. Peifer, S. Ramaswamy, N. Sano, P. G. Scrobohaci, S. Selberherr, M. Takenaka, T. Tang, J. L. Thobel, R. Thoma, K. Tomizawa, M. Tomizawa, T. Vogelsang, S. Wang, X. Wang, C.Yao, P. D. Yoder, and A. Yoshii: IEEE Trans. Electron Devices **41** (1994) 1646.

4. M. V. Fischetti, S. E. Laux, and E. Crabbe: J. Appl. Phys. **78** (1995) 1058.
5. F. M. Bufler: Dissertation, Universität Bremen, Bremen, 1997.
6. M. M. Rieger and P. Vogl: Phys. Rev. B **48** (1993) 14276.
7. E. X. Wang, M. D. Giles, S. Yu, F. A. Leon, A. Hiroki, and S. Odanaka: *Proc. SISPAD* No. 1 (1996) p.67.
8. R. Thoma, A. Emunds, B. Meinerzhagen, H. J. Peifer, and W. L. Engl: IEEE Trans. Electron Devices **38** (1991) 1343.
9. W. Brauer and H. W. Streitwolf, *Theoretische Grundlagen der Halbleiterphysik* (Vieweg, Braunschweig, 1977) 2nd ed.
10. O. Madelung, *Introduction to Solid State Theory* (Springer, Berlin, 1978).
11. R. Stratton: Phys. Rev. **126** (1962) 2002.
12. C. Jungemann, S. Yamaguchi, and H. Goto: IEEE J. Tech. Comp. Aided Design **10** (1998).
13. H. Nakagawa and S. Zukotynski: Can. J. Phys. **56** (1978) 364.
14. M. L Cohen and T.K. Bergstresser: Phys. Rev. **141** (1966) 789.
15. P. Gaworzewski, K. Tittelbach-Helmrich, U. Penner, and N. V. Abrosimov: J. Appl. Phys. **83** (1998) 5258.